Title Page

Targeting the Cannabinoid Receptor CB2 in a Mouse Model of l-dopa Induced Dyskinesia

Author names and affiliations

Peggy Rentsch [a,b,c], Sandy Stayte [a,c], Timothy Egan [a,c], Ian Clark[d], Bryce Vissel [a,c]

[a] Centre for Neuroscience and Regenerative Medicine, Faculty of Science, University of Technology Sydney, 15 Broadway, 2007, Sydney, NSW, Australia

[b] Faculty of Medicine, University of New South Wales, High Street, 2052, Sydney, NSW, Australia

[c] St. Vincent's Centre for Applied Medical Research (AMR), 405 Liverpool St, 2010, Sydney, NSW, Australia

[d] Research School of Biology, Australian National University, Canberra, ACT, Australia

Corresponding Author

Professor Bryce Vissel

Mailing: Faculty of Science, UTS, PO Box 123 Broadway NSW 2007

Mobile: +61 412 522 148

E-mail: bryce.vissel@uts.edu.au

Abstract

L-dopa induced dyskinesia (LID) is a debilitating side-effect of the primary treatment used in Parkinson's disease (PD), l-dopa. Here we investigate the effect of HU-308, a cannabinoid CB2 receptor agonist, on LIDs. Utilizing a mouse model of PD and LIDs, induced by 6-OHDA and subsequent l-dopa treatment, we show that HU-308 reduced LIDs as effectively as amantadine, the current frontline treatment. Furthermore, treatment with HU-308 plus amantadine resulted in a greater anti-dyskinetic effect than maximally achieved with HU-308 alone, potentially suggesting a synergistic effect of these two treatments. Lastly, we demonstrated that treatment with HU-308 and amantadine either alone, or in combination, decreased striatal neuroinflammation, a mechanism which has been suggested to contribute to LIDs. Taken together, our results suggest pharmacological treatments with CB2 agonists merit further investigation as therapies for LIDs in PD patients. Furthermore, since CB2 receptors are thought to be primarily expressed on, and signal through, glia, our data provide weight to suggestion that neuroinflammation, or more specifically, altered glial function, plays a role in development of LIDs.

Keywords

6-OHDA; Abnormal involuntary movements; CB2; Cannabinoids; Dyskinesia; l-dopa; Neuroinflammation; Parkinson's disease; Striatum

Abbreviations

6-OHDA, 6-hydroxydopamine; AIM, abnormal involuntary movement; CB, cannabinoid receptor; GFAP, glial fibrillary acidic protein; IBA1, ionized calcium binding adaptor molecule 1; IL-1β, interleukin-1beta; IL-6, interleukin-6; IL-10, interleukin-10; LID, l-dopa induced dyskinesia; MFB, medial forebrain bundle; NF-κB, nuclear factor kappa-light-chain-enhancer of activated B cells; PBS, phosphate buffered saline; PD, Parkinson's disease; SEM, standard error of the mean; SNpc, substantia nigra pars compacta; TNF, tumor necrosis factor; TH, tyrosine hydrolase

1. Introduction

Parkinson's disease (PD) is a neurodegenerative disorder caused by the progressive loss of dopaminergic neurons in the substantia nigra pars compacta (SNpc) and their projections into the striatum. As PD progresses dopamine availability decreases, leading to the characteristic locomotor deficits including tremors, rigidity and bradykinesia (Chaudhuri et al., 2006). For several decades dopamine replacement therapy with l-dopa has been the gold-standard treatment for combating the motor symptoms for patients with PD. However, as disease progresses, l-dopa doses often need to be increased in order to manage symptoms. Approximately 52-78% of patients may in turn develop debilitating l-dopa induced dyskinesias (LIDs), classified as abnormalities or impairments of voluntary movements, within 10 years of initiating treatment (Manson et al., 2012). Accordingly, LIDs present a clinical-therapeutic conundrum, as the appearance of LIDs prevents further increasing l-dopa doses and in fact often needs to be managed by lowering l-dopa doses, which in turn leads to the loss of l-dopa's anti-parkinsonian efficacy (Pandey and Srivanitchapoom, 2017).

To date, the only FDA approved therapy to combat LIDs in PD patients is amantadine. The clinical use of amantadine is unfortunately limited by several side effects, the development of tolerance and a lack of efficacy in some patients (Perez-Lloret and Rascol, 2018; Sharma et al., 2018). For this reason, there is a great unmet clinical need for new therapies to treat LIDs.

In order to develop new therapies for LIDs, it is necessary to target the underlying mechanisms. Amantadine has been thought to exert its beneficial effects through its weak NMDA receptor antagonism at synapses (Blanpied et al., 2005; Paquette et al.,

2012), while recent research has intriguingly identified amantadine's effects on glia as a potential mechanism (Kim et al., 2012; Ossola et al., 2011). More generally, while there is no consensus, synapse loss and pathological regrowth (Fieblinger et al., 2014; Suárez et al., 2014; Zhang et al., 2013), changes in synaptic plasticity (Picconi et al., 2003; Thiele et al., 2014) and neuroinflammation (Mulas et al., 2016), have all been implicated in LID pathogenesis. Given the growing understanding of the enumerate roles of glia in the healthy and diseased brain (Hammond et al., 2018; Khakh and Sofroniew, 2015; Morris et al., 2013) including LIDs (Mulas et al., 2016), targeting neuroinflammation, or perhaps more specifically glial signaling, provides a potential strategy for pre-clinical and clinical drug development for LIDs.

If targeting neuroinflammation, and or glial signaling, offers a potential strategy, then cannabinoid based therapies could be an option for treating LIDs. Cannabinoid-based therapies can exert effects on glia, are thought to suppress neuroinflammation, and have neuroprotective effects in preclinical animal models of several neurodegenerative disorders (Bisogno and Di Marzo, 2010). Intriguingly, some observational studies have indicated that smoking medical cannabis can alleviate LID in PD patients (Finseth et al., 2015; Lotan et al., 2014; Venderová et al., 2004). Cannabinoid effects are primarily mediated through the cannabinoid receptors CB1 and CB2 and previous preclinical studies have demonstrated that CB1 agonists (dos-Santos-Pereira et al., 2016; Ferrer et al., 2003; Fox et al., 2002; Martinez et al., 2012; Morgese et al., 2007; Song et al., 2014; Walsh et al., 2010) exert anti-dyskinetic properties. In contrast, the therapeutic potential of exclusively targeting CB2 receptors has not yet been investigated.

While CB2 selective agonists have not been investigated, they could be of particular clinical relevance, as it is suggested that targeting this receptor does not provoke the psychoactive side-effects associated with CB1 receptor activation (Pacher et al., 2006). Moreover, in the brain CB2 receptors are thought to be predominantly expressed by microglia (Jordan and Xi, 2019; Palazuelos et al., 2009) and astrocytes (Fernández-Trapero et al., 2017). Further, while CB2 expression in the healthy brain is relatively low, expression in glia is elevated in preclinical animal models of neurodegenerative diseases as well as in human brain tissue of Parkinson's (Gómez-Gálvez et al., 2016), Huntington's (Palazuelos et al., 2009) and Alzheimer's disease patients (Benito et al., 2003). One intriguing interpretation of this is that CB2 expression is upregulated as part of a glial homeostatic response. In support of this, CB2 receptor activation appears to initiate a signalling cascade in glia leading to decreased pro-inflammatory cytokine production and decreased glial cell-proliferation (Ashton and Glass, 2007). These effects are hypothesised to contribute to neuroprotection in various toxin based rodent models of PD including rotenone (Javed et al., 2016), MPTP (Price et al., 2009) and LPS (Gómez-Gálvez et al., 2016). Thus, pharmacologically stimulating CB2 receptor signalling may be a promising therapeutic strategy for neurodegenerative conditions where neuroinflammation, and therefore altered glial responses (Ben Haim et al., 2015; Booth et al., 2017; Morris et al., 2013; Priller and Prinz, 2019), are implicated.

Collectively, the apparent potential of cannabinoid therapies for treatment of several neurological conditions (Benito et al., 2003; Gómez-Gálvez et al., 2016; Palazuelos et al., 2009), the putative relationship of neuroinflammation in LID pathogenesis (Mulas et al., 2016), the expression of CB2 in glia and their stated anti-inflammatory

properties (Gómez-Gálvez et al., 2016; Javed et al., 2016; Price et al., 2009), all point to CB2 receptors as a promising therapeutic target for dyskinesia. Thus, in the current study, we hypothesized that a CB2 receptor agonist may exert anti-dyskinetic efficacy in a mouse model of LID.

To test this hypothesis, we utilized the selective CB2 receptor agonist HU-308 (Hanus et al., 1999). HU-308 treatment has previously been shown to reduce microglia proliferation and cytokine expression and provide concurrent neuroprotection in mouse models of Parkinson's (Gómez-Gálvez et al., 2016) and Huntington's disease (Palazuelos et al., 2009). We aimed to determine if the putative actions of HU-308 on glia could also translate into an effect on LIDs created by repeat l-dopa treatment in a 6-OHDA mouse model of PD. We also investigated the potential anti-dyskinetic effect of HU-308 alone and in combination with amantadine, as well as their effects on glial reactivity in striatal tissue of 6-OHDA lesioned mice expressing LIDs.

2. Material and methods

2.1 Animals

Male C57BL/6j mice aged 7-11 weeks were obtained from Australian BioResources (Mona Vale, Australia) and were allowed to acclimatize for one week prior to study commencement. Mice were housed at a maximum five mice per cage, until the study began, at which time mice were housed individually. Mice were kept on a 12-hour light/dark cycle with access to food and water *ad libitum*. All animal experiments were performed with the approval of the Garvan Institute and St. Vincent's Hospital Animal Ethics Committee under approval numbers 12/36 and 15/38 in accordance

with National Health and Medical Research Council animal experimentation guidelines and the Australian Code of Practice for the Care and Use of Animals for Scientific Purposes (2004). All surgeries were performed under ketamine/xylazil anaesthesia, and all efforts were made to minimize suffering.

2.2 Unilateral medial forebrain bundle (MFB) lesioning

Thirty minutes prior to surgery desipramine hydrochloride (Sigma Aldrich) was administered at 10 ml/kg by intra-peritoneal (i.p.) injection. Animals were then anaesthetized with a mixture of ketamine (8.7 mg/ml; Mavlab) and xylazil (2 mg/ml; Troy Laboratories Pty Ltd) and placed in stereotaxic apparatus (Kopf Instruments). Mice were then injected with 0.2 µl of 15 mg/ml (total 3 µg) of 6-hydroxydopamine hydrobromide (Sigma Aldrich) in 0.02% ascorbic acid in the right MFB at the following coordinates: AP -1.2, ML -1.1, DV -5.0, relative to bregma and the dural surface, as previously described (Rentsch et al., 2019; Thiele et al., 2012). 6-OHDA (or 0.02% ascorbic acid control) was injected at a rate of 0.1 µl/minute and the syringe was left in place for 5 minutes following each injection to allow for complete diffusion into the target area. The incision was sutured (Dynek) and animals were placed in individual cages on heating pads. During post-operative recovery, mice were provided with recovery gels and sugared milk to ensure adequate nutrition and hydration. One half of the cage was kept on heading pads for the entire study, to allow mice to choose their environment and to preclude hypothermia. Mice were monitored daily for three weeks following surgery and were injected subcutaneously with 300 µl glucose (5%) and 300 µl saline (0.9%) (Schuler et al., 2009) if signs of dehydration and malnutrition were present.

2.3 Cylinder test

Mice were placed into a clear circular cylinder (diameter 15cm) on three occasions (prior to 6-OHDA lesion surgery, 3 weeks post 6-OHDA lesion surgery, 3 weeks and 1 day post 6-OHDA lesion surgery after receiving initial treatment and l-dopa injection) and the first 20 paw placements of the left or right paw on the cylinder wall were scored. Only full juxtapositions of the paw to the cylinder wall were counted that served the purpose of supporting the animal's body weight. The total forelimb bias was determined by calculating the number of wall contacts made with the impaired paw (left) as a percentage of total contacts. The cylinder was cleaned with 70% ethanol between animals.

2.4 Abnormal involuntary movements (AIMs)

Mice were co-administered with l-dopa methyl ester (6 mg/kg; Sigma Aldrich, in saline i.p.) and benserazide-HCl (12.5 mg/kg; Sigma Aldrich, in saline i.p.) to induce abnormal involuntary movements (AIMs) as described in the experimental design. AIMs were evaluated according to the mouse dyskinesia scale described in detail previously (Cenci and Lundblad, 2007; Rentsch et al., 2019; Sebastianutto et al., 2016). Briefly, mice were placed individually in transparent plastic cylinders (diameter 15 cm) without bedding material and scored for 1 min every 20th min during the 120 min following l-dopa administration. The AIMs were classified into three subtypes according to their topographic distribution. Axial AIMs were characterized by twisting motions of the neck and upper trunk towards the contralateral side of the lesion. Limb AIMs are rapid uncontrolled movements or dystonic posturing of the contralateral forelimb and orolingual AIMs are movements affecting orofacial muscles and contralateral tongue protrusion. AIMs

were scored on two different parameters simultaneously on a scale of 1-4 (with 4 being the highest) based on the severity (amplitude scale) and the amount of time they are present (basic scale). A total AIM score was then produced by multiplying basic score and amplitude score for each AIM subtype, at each monitoring period, and the sum of these scores is referred to as “global AIMs”.

2.5 Immunohistochemistry

Brains were harvested and processed as described in detail previously (Stayte et al., 2015). 40 µm coronal brain sections were blocked with 3% BSA + 0.25% Triton-X-100 and then incubated in the following primary antibodies: polyclonal rabbit ionized calcium binding adaptor molecule 1 (IBA1, 1:1000 Novachem, cat # 019-19741), monoclonal mouse glial fibrillary acidic protein (GFAP 1:500, Cell signalling, cat # 3670) monoclonal mouse tyrosine hydroxylase (TH, 1:1000 Sigma Aldrich, cat # T2928), or polyclonal rabbit anti-TH (1:1000, Merck Millipore, cat # AB152) for 72 hours at 4°C. All sections were then incubated in their respective secondary antibodies (1:250, Invitrogen, cat # A11029, A11008, A21236, A21245) overnight at 4°C followed by a counterstain with 4’,6-diamidino-2-phenylindole (DAPI; Life Technologies). Finally, sections were mounted onto SuperFrost-plus slides (Menzel-Glaser) and coverslipped with 50% glycerol mounting medium (Merck).

2.6 Stereology

Striatal cell populations were quantified using the optical fractionator method and Stereo Investigator 7 software (MBF Bioscience), as previously described (Stayte et al., 2015). For estimations of IBA1 positive populations a counting frame of 100 µm x 100 µm and a grid size of 333 µm x 333 µm was used, while for the estimations of

GFAP positive populations a counting frame of 120 µm x 120 µm and a grid size of 300 µm x 300 µm was used. For all cell types the guard zone height used was 5 µm and dissector height used was 10 µm, with every 12th section sampled to a total of 7 sections. Coefficient of error attributable to the sampling was calculated according to Gundersen and Jensen (Gundersen and Jensen, 1987). Errors ≤0.10 were regarded as acceptable. The striatum was delineated from -1.53 to 1.35 mm relative to bregma based on the Paxinos atlas for the mouse brain and divided into two subregions, the dorsal-lateral and ventral-medial striatum (Paxinos and Franklin, 2001). In order to ensure that differences in glial counts did not originate from differences in tracing volume these data are presented as number of cells per area instead of absolute numbers.

2.7 Capillary western blotting (Wes)

Striatal tissue homogenates and protein quantification were performed as previously described (Stayte et al., 2017). Western blotting analysis was performed using the capillary automated Wes system (ProteinSimple). Using the Wes12–230kDa separation module (ProteinSimple, SM-W004) samples were prepared according to manufacturer's instructions and the following primary antibodies were utilized: monoclonal mouse FosB (1:100 Abcam, cat # ab11959), polyclonal rabbit anti-TH (1:1000, Merck Millipore, cat # AB152), monoclonal rabbit nuclear factor kappa-light-chain-enhancer of activated B cells (NF-κB, 1:100 Cell signalling, cat # 4764), monoclonal rabbit NF-κB (Ser536) (1:10 Cell signalling, cat # 3033), monoclonal mouse beta-tubulin (1:1000 Promega, cat # G712A) and monoclonal mouse glyceraldehyde 3-phosphate dehydrogenase (GAPDH, 1:5000 Abcam, cat # ab8245). For protein detection the anti-rabbit detection module (ProteinSimple, DM-

001) or the anti-mouse detection module (ProteinSimple, DM-002) was used and for multiplexing the concentrated 20x anti-rabbit (ProteinSimple, 043426) was used in combination with the anti-mouse detection module. Data were analysed using the Compass software and peak area measurements were obtained for the protein of interest and normalized to the biological loading control.

2.8 Bead based immune assay

Using the same striatal tissue sample as for the western blotting analysis, tumor necrosis factor alpha (TNFα), interleukin-1beta (IL-1β), interleukin-6 (IL-6) and interleukin-10 (IL-10) cytokine levels were quantitatively measured by the BD cytometric bead array mouse enhanced Kit (BD Bioscience). The operations were performed according to the manufacturer's instructions utilizing a LSR-II flow cytometer (Becton Dickinson) with FACSDiva software and FCAP array software.

2.9 Statistics

All statistical analyses were performed using IBM SPSS Statistics version 25 (SPSS Inc.) or Prism 6 (GraphPad). Shapiro-Wilk tests were performed on all data sets to assess normality, before analysing data either with parametric or non-parametric tests. For normally distributed data, differences between means were assessed, as appropriate, by one- or two- way ANOVA with or without repeated measures, followed by Bonferroni *post hoc* analysis. All data is presented as mean ± standard error of the mean (SEM). For all statistical tests, a p value of ≤ 0.05 was assumed to be significant.

2.10 Experimental design

Beginning three weeks following 6-OHDA lesion surgery animals received repeated l-dopa and benserazide injections over a three week period. During the final week AIMs were scored on two occasions (Pretest). Animals that failed to develop AIMs (global AIMs score below 40) or that, post study, had an insufficient lesion (less than 60% loss of TH in ipsilateral striatum when compared to contralateral hemisphere) were excluded from the study. Based on the AIM scores of the two testing sessions animals were equally divided into treatment groups. Beginning the day after the last pretest animals started to receive daily i.p treatment injections (40mg/kg amantadine (Sigma Aldrich); 1mg/kg, 2.5mg/kg or 5mg/kg HU-308 (Tocris); 1mg/kg SR144528 (Sigma Aldrich)). All drugs were dissolved in Tween 80 and dimethyl sulfoxide (DMSO), and then diluted in saline (Tween 80:DMSO:saline = 1:1:18). 30 min after treatment injections animals were injected with l-dopa and benserazide. AIM expression was measured every third day for a total of five testing sessions. On the day after the last AIM scoring session animals received a final l-dopa/benserazide injection and tissue was collected 1h later (Fig. 1A). For all immunohistochemical experiments animals were anaesthetized via a ketamine/xylazil mixture before cardiac perfusion with 4% paraformaldehyde. For all other analyses animals were anaesthetized via isofluorane followed by cervical dislocation and rapid tissue collection. The experimenter was at all times blinded to group assignment and outcome assignment in every experiment performed and tissue collection and processing was performed in appropriate blocks. All experiments were performed in at least two separate trials with at least three replicates per group (Fig. 1B).

A

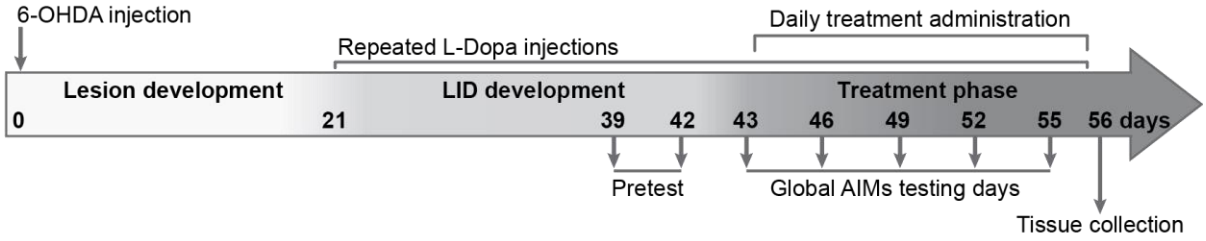

B

Experiment	Trial	Mortality	Exclusion criteria		# of mice per group used for analysis			
			AIM score	Lesion success	AIMs scoring	IHC	WB	Cytokine measurements
HU-308 dose (Figure 2)	1	15%	0	0	6	-	3	-
	2	51%	0	0	6	-	3	-
	3	0%	0	0	3	-	3	-
CB2 specificity (Figure 3)	1	5%	2	0	5	-	4	-
	2	9%	0	0	5	-	4	-
Amantadine and HU-308 (Figure 4-7)	1	6%	3	1	4	3	-	-
	2	6%	2	0	3	3	-	-
	3	8%	3	0	5	-	5	5
	4	11%	0	0	-	-	3	3

Figure 1: Experimental design. (A) Timeline of the study. (B) List of experiments performed, including the number of trials, respective mortality, the number of animals excluded from the study and the number of animals per treatment group used for behavioural and molecular analysis.

3. Results

3.1 A CB2 agonist, HU-308, has a behavioural effect on LIDs

3.1.1 HU-308 dose-dependently decreased the severity of LID in mice

HU-308 has previously been shown to exert its anti-inflammatory and neuroprotective effects in rodent models of Parkinson's (Gómez-Gálvez et al., 2016) and Huntington's disease (Palazuelos et al., 2009) at a dose of 5mg/kg. Using this

dose as a starting point, we first intended to test the dose-dependent efficacy of HU-308 on reducing established AIMs in 6-OHDA lesioned mice.

A two-way repeated measures ANOVA revealed a significant interaction ($F_{(12,224)}$=3.546, p<0.001; Fig. 2A) between dosage and time point, indicating a dose dependent effect that changes over time. The simple effect was significant for dose ($F_{(3,56)}$=10.49, p<0.001) and time ($F_{(4,224)}$=17.63, p<0.001). Post hoc analysis revealed that 2.5mg/kg (day 1 – day 13 p<0.001) and 5mg/kg (day 1 – day 10 p<0.001; day 13 p<0.01) significantly reduce AIMs when compared to the control at each time point. In contrast the 1mg/kg dose only showed a trend towards reduction of AIMs, but no sustained statistically significant anti-dyskinetic effect over the course of treatment. Collectively, our behavioural results indicate an anti-dyskinetic effect of 2.5mg/kg and 5mg/kg HU-308, with the maximal effect not increasing beyond that seen at 2.5mg/kg. Importantly, this anti-dyskinetic effect of HU-308 did not occur at the expense of the anti-parkinsonian efficacy of l-dopa, as forelimb use asymmetry, evaluated using the cylinder test (Schallert et al., 2000), was improved by l-dopa alone or when co-administered with HU-308 (t-test: Pre-lesion p=0.2936; 6-OHDA lesion p=0.7885; 6-OHDA lesion + 1. L-Dopa p>0.9999; Fig. 2B).

Molecular analysis of FosB, a protein widely used as a molecular marker of LIDs (Andersson et al., 1999; Winkler et al., 2002), largely confirmed our behavioural findings. A one-way ANOVA revealed a significant reduction of striatal FosB expression following HU-308 treatment ($F_{(3,32)}$=12.74, p<0.001; Fig. 2C). Bonferroni post hoc analysis indicated a similar reduction of FosB expression for 1mg/kg (p<0.001), 2.5mg/kg (p<0.001) and 5mg/kg (p<0.01) treatment groups when

compared to control. Lastly, to rule out the possibility of different lesion sizes to explain any anti-dyskinetic effects, we quantified TH protein levels in both the lesioned and non-lesioned striatum. A two-way ANOVA of hemisphere and treatment on TH expression revealed that all mice had a similar unilateral lesion size that was not affected by treatment regime (interaction $F_{(3,64)}$=0.3106, p=0.8176, hemisphere $F_{(1,64)}$=384.6, p<0.001, treatment $F_{(3,64)}$=0.3372, p=0.7984; Fig. 2D). Collectively, these results indicate 2.5mg/kg HU-308 as the lowest effective dose exerting a behavioural anti-dyskinetic effect that is supported with a reduction in FosB expression. Given there was no increased benefit of 5mg/kg HU-308, the 2.5mg/kg dose was used in subsequent experiments.

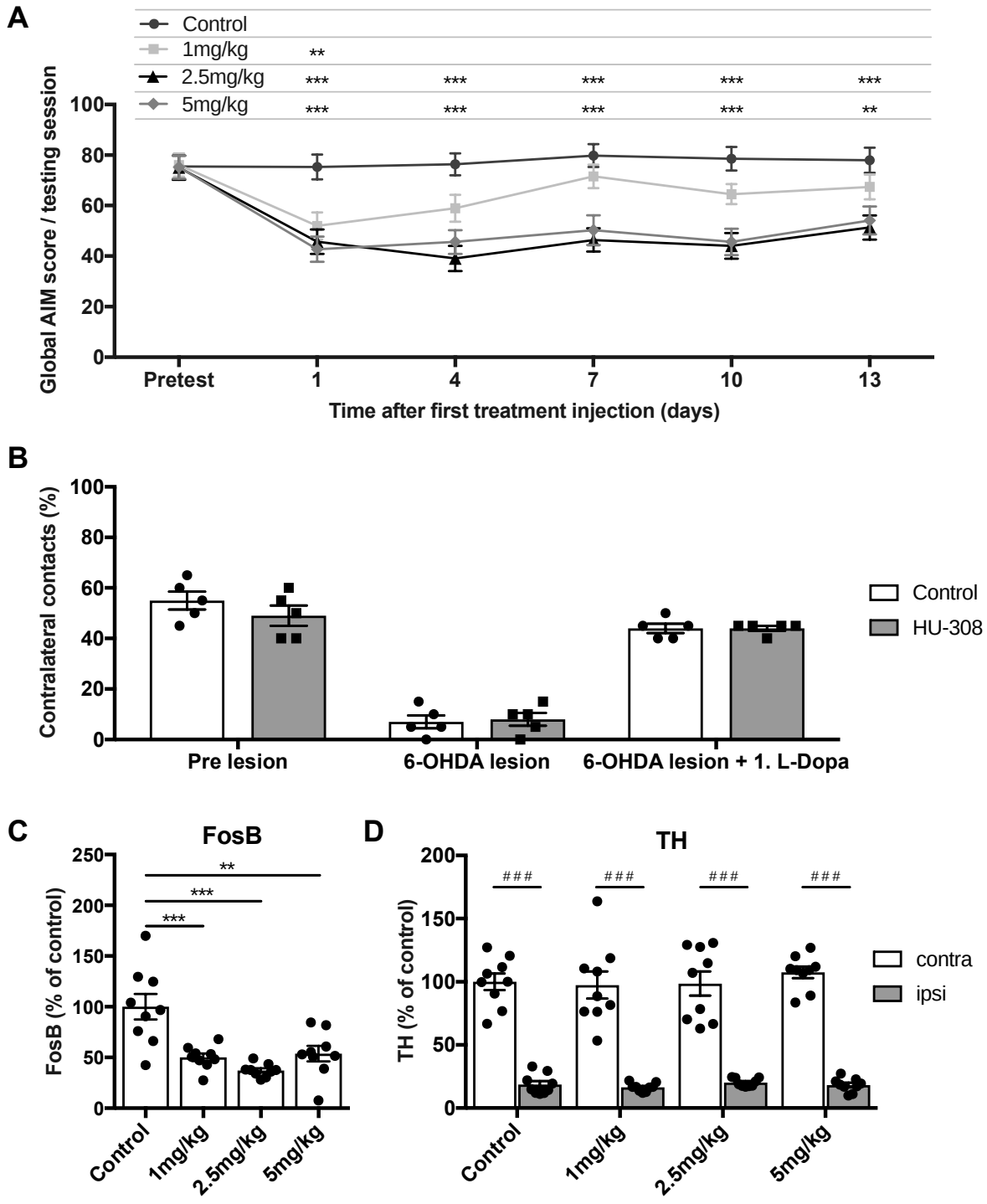

298

299 **Figure 2: HU-308 dose-dependently attenuates LIDs.** (A) Systemic treatment with
300 2.5mg/kg and 5mg/kg HU-308 produced a significant reduction in global AIM scores
301 over the entire testing period of 13 days, whereas 1mg/kg HU-308 alleviated AIMs
302 on the first day with only a trend to effect seen subsequently when compared to the
303 control (n = 15 per group). (B) Cylinder test demonstrated that 2.5mg/kg HU-308 did

not affect the anti-parkinsonian efficacy of L-Dopa treatment (n = 5 per group). Western blotting analysis revealed (C) reduced FosB expression in the ipsilateral striatum at every dose when compared to the control and (D) TH expression was consistently reduced in the ipsilateral striatum when compared to the contralateral hemisphere at every dose (n = 9 per group). All values represent the mean ± SEM. ** = p < 0.01, *** = p <0.001 compared to control; ### = p < 0.001 compared to contralateral hemisphere.

3.1.2 The anti-dyskinetic effect of HU-308 can be eliminated with a CB2 antagonist

After establishing that HU-308 reduced LID severity we next aimed to investigate the CB2 receptor specificity of this effect. To determine this in the following experiment we co-administered HU-308 with the selective CB2 receptor antagonist SR144528 (Hanus et al., 1999), to determine whether this could block the anti-dyskinetic effect of HU-308. Furthermore we analysed the effect of CB2 antagonism on LIDs, alone.

A two-way repeated measures ANOVA revealed no significant interaction ($F_{(12,144)}$=0.536, p=0.8883; Fig. 3A) between treatment and time point, with no main effect of time ($F_{4,144)}$=2.354, p=0.0567), but a significant effect of treatment ($F_{(3,36)}$=33.02, p<0.001). Post-hoc analysis confirmed the ability of HU-308 (p<0.001) to significantly reduce AIMs, as reported above. SR144528 (p>0.999) had no effect on AIMs when administered alone, however when mice were treated with HU-308 and SR144528 conjointly, SR144528 abolished the anti-dyskinetic effect of HU-308 (p<0.001), indicating the CB2 specificity of HU-308 treatment. These behavioural

data are strongly supported with the molecular analysis of FosB protein in striatal tissue. A one way ANOVA revealed a significant effect of FosB expression ($F_{(3,28)}$=3.951, p<0.05; Fig. 3B). Bonferroni post-hoc analysis indicated a reduction of FosB expression in HU-308 treated animals (p<0.05) however this effect was lost in animals that were co-administered with HU-308 and SR144528. In summary, these behavioural and molecular results indicate the importance of CB2 signalling in the anti-dyskinetic effect of HU-308. Lastly, a two-way ANOVA of hemisphere and treatment on TH expression confirmed that all mice had a stable unilateral lesion that was not affected by treatment regime (interaction $F_{(3,56)}$=3.399 p=0.0239, hemisphere $F_{(1,56)}$=732.1, p<0.001, treatment $F_{(3,56)}$=2.397, p=0.0777; Fig. 3C).

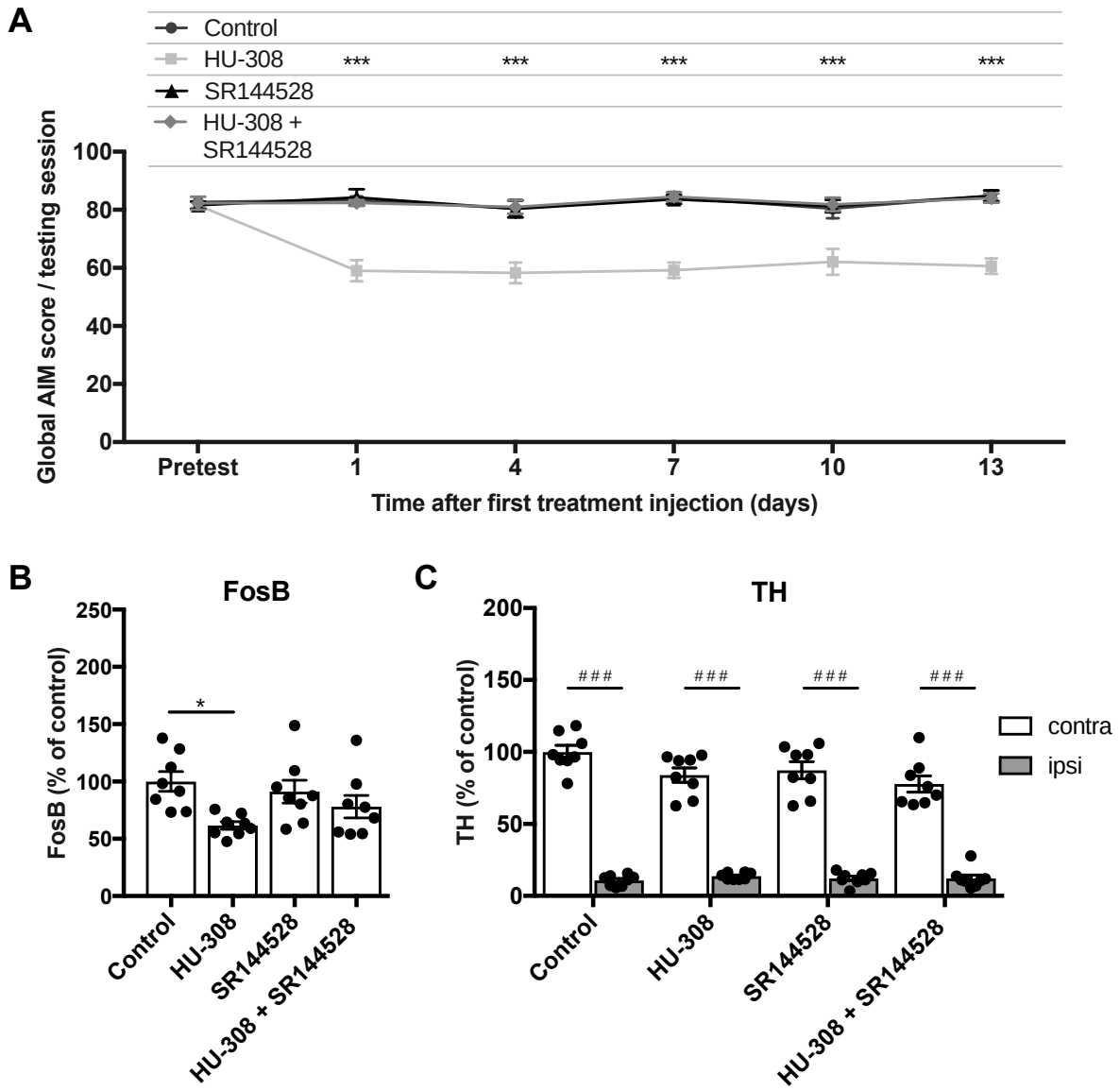

338

339 **Figure 3: SR144528 blocks the anti-dyskinetic effect of HU-308.** The efficacy of
340 HU-308 (2.5mg/kg) on reducing (A) AIMs (n = 10 per group) and (B) FosB
341 expression (n = 8 per group) is inhibited when co-administered with the CB2
342 antagonist SR144528 (1mg/kg). (C) TH expression was consistently reduced in the
343 ipsilateral striatum when compared to the contralateral hemisphere with every
344 treatment (n = 8 per group). All values represent the mean ± SEM. * = $p < 0.05$, *** =
345 $p < 0.001$ compared to control; ### = $p < 0.001$ compared to contralateral
346 hemisphere.

3.1.3 The combined treatment of HU-308 and amantadine resulted in an additive anti-dyskinetic effect

Next we aimed to compare the magnitude of the anti-dyskinetic effect of HU-308 to that of amantadine. We also aimed to investigate the possibility of an additive anti-dyskinetic effect of amantadine and HU-308 co-treatment.

A two-way repeated measures ANOVA revealed no significant interaction ($F_{(12,176)}$=0.9064, p=0.5418; Fig. 4A) between treatment and time, with a minor main effect of time ($F_{(4,176)}$=2.484, p<0.05) and a strong significant effect of treatment ($F_{(3,44)}$=28.34, p<0.001). Post-hoc analysis indicated that HU-308 treatment (p<0.001) was as effective as amantadine (p<0.001) in reducing AIMs when compared to the control. Strikingly, the combined treatment of amantadine and HU-308 was not only significantly more effective than the control (p<0.001), but also more effective than the individual amantadine (p<0.01) and HU-308 (p<0.01) treatment groups. This may suggest a synergistic effect of the combined treatment regime.

Next, we performed a detailed analysis of individual time points on the first day (Day 43) and the last day (Day 55) of treatment, in order to elucidate if these treatment regimes shorten the time or reduce the severity of AIMs expression. Two-way repeated measures ANOVAs revealed significant interaction (Day 43: $F_{(15,220)}$=5.376, p<0.001; Day 55: $F_{(15,220)}$=4.385, p<0.001; Fig. 2B/C) between treatment and time. Therefore the simple effects were analysed and were significant for time (Day 43: $F_{(5,220)}$=342.7, p<0.001; Day 55: $F_{(5,220)}$=484.2 , p<0.001) and treatment (Day 43:

$F_{(3,44)}$=21.45, p<0.001; Day 55: $F_{(3,44)}$=18.5, p<0.001). Post-hoc analysis revealed that all treatments reduced the severity of AIMs at peak LID (20-80min) when compared to the control and combined treatment of amantadine and HU-308 was more effective than the individual amantadine and HU-308 treatment groups, further favouring the hypothesis of a synergistic effect.

Additionally, a one way ANOVA of FosB expression revealed a significant effect ($F_{(3,28)}$=8.821, p<0.001; Fig. 4D), supporting our behavioural findings. Bonferroni post-hoc analysis indicated a reduction of FosB expression in amantadine (p<0.001), HU-308 (p<0.01) and amantadine + HU-308 (p<0.01) when compared to control. Lastly, a two-way ANOVA of hemisphere and treatment on TH expression revealed that all mice had a stable unilateral lesion that was not affected by treatment regime (interaction $F_{(3,56)}$=0.4353 p=0.7286, hemisphere $F_{(1,56)}$=735.9, p<0.001, treatment $F_{(3,56)}$=0.2472, p=0.8630; Fig. 4E).

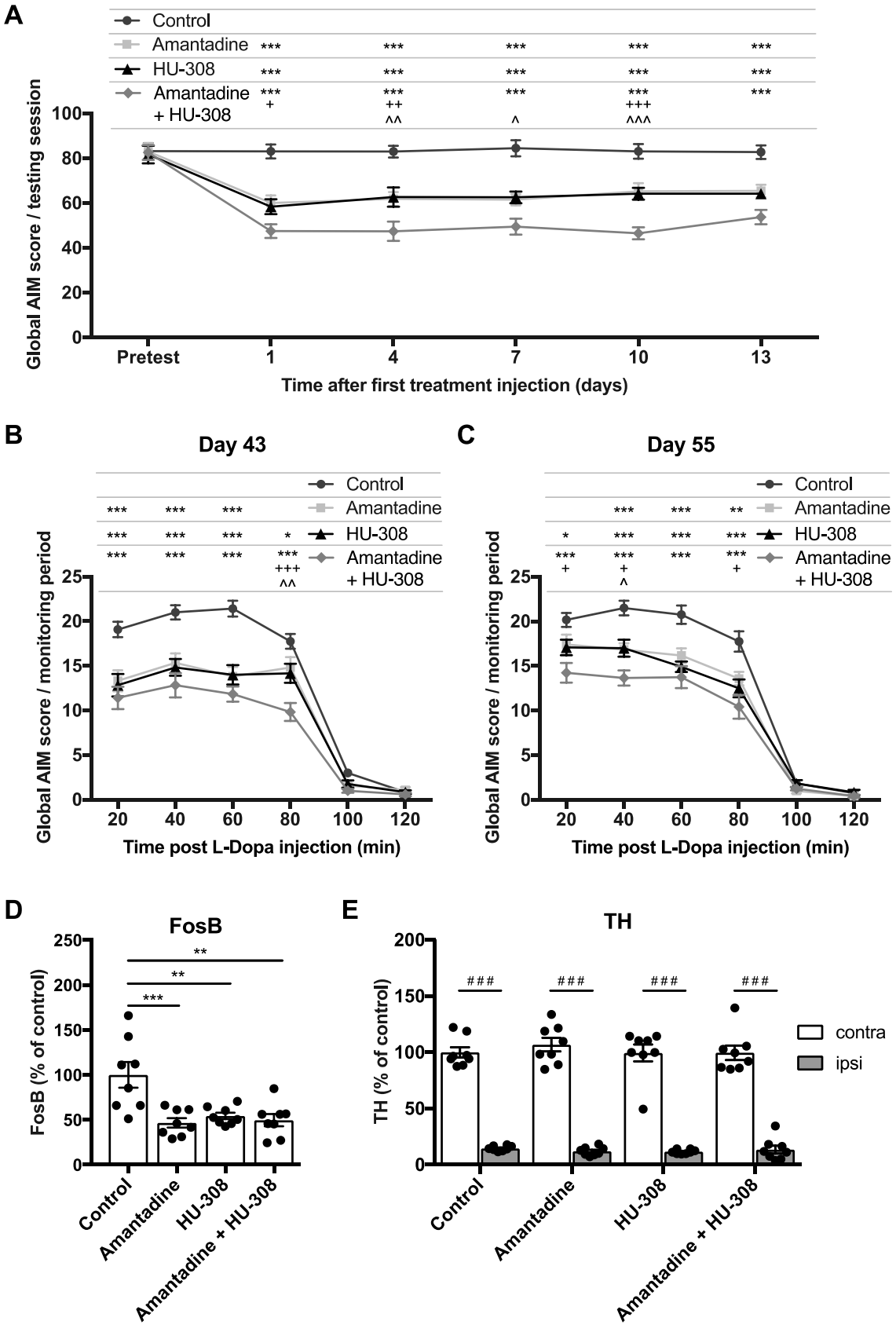
A
Control
Amantadine
HU-308
Amantadine + HU-308
Global AIM score / testing session
Pretest
1
4
7
10
13
Time after first treatment injection (days)
B
Day 43
Global AIM score / monitoring period
Time post L-Dopa injection (min)
C
Day 55
Global AIM score / monitoring period
Time post L-Dopa injection (min)
D
FosB
FosB (% of control)
Control
Amantadine
HU-308
Amantadine + HU-308
E
TH
TH (% of control)
contra
ipsi
Control
Amantadine
HU-308
Amantadine + HU-308

386

Figure 4: Treatment with amantadine plus HU-308 results in an additive anti-dyskinetic behavioural effect. Systemic treatment with amantadine (40mg/kg) and HU-308 (2.5mg/kg) resulted in a similar reduction in global AIM scores and conjoint treatment enhanced this anti-dyskinetic effect (n = 12 per group) over (A) five testing sessions and during each monitoring session on (B) day 43 and (C) day 55. Western blotting analysis revealed (D) reduced FosB expression in the ipsilateral striatum with every treatment regime when compared to the control (n = 8 per group) and (E) TH expression was consistently reduced in the ipsilateral striatum when compared to the contralateral hemisphere with every treatment (n = 8 per group). All values represent the mean ± SEM. ** = $p < 0.01$, *** = $p < 0.001$ compared to control; + = $p < 0.05$, ++ = $p < 0.01$, +++ = $p < 0.001$ compared to amantadine; ^ = $p < 0.05$, ^^ = $p < 0.01$, ^^^ = $p < 0.001$ compared to HU-308; ### = $p < 0.001$ compared to contralateral hemisphere.

3.2 Both HU-308 and amantadine reduce neuroinflammation in the striatum of dyskinetic mice

Having established a robust anti-dyskinetic effect of amantadine and HU-308 treatment we next aimed to investigate a possible underlying mechanism. Both amantadine (Kim et al., 2012; Ossola et al., 2011) and HU-308 (Gómez-Gálvez et al., 2016; Palazuelos et al., 2009) have previously been reported to reduce pro-inflammatory markers as well as reducing glial proliferation. Since neuroinflammation, which is associated with changes in glial morphology and signalling, has previously been linked to LIDs (Mulas et al., 2016), we aimed to investigate if our treatment regimes influence glial proliferation and neuroinflammatory signalling.

3.2.1 Amantadine and HU-308 reduce microglia and astrocyte populations in the striatum of 6-OHDA lesioned mice

As some research indicates the dorsal-lateral striatum as the most important striatal subregion associated with changes in LIDs (Fasano et al., 2010; Girasole et al., 2018; Pavón et al., 2006), we set out to assess if HU-308 and/or amantadine reduced microglial and astrocyte populations in the dorsal-lateral and ventral-medial striatum.

To quantify microglial numbers we counted IBA1 positive cells, a widely used marker to label microglia populations. One-way ANOVA analyses revealed significant differences of IBA1 positive cells between treatment groups in the dorsal-lateral ($F_{(3,20)}$=7.317, p<0.01; Fig. 5B) and ventral-medial ($F_{(3,20)}$=15.66, p<0.001; Fig. 5C) striatum. Post hoc analyses demonstrated that IBA1 positive cells were decreased in amantadine (DL: p<0.05; VM: p<0.001), HU-308 (DL: p<0.01; VM: p<0.001) and amantadine + HU-308 (DL: p<0.05; VM: p<0.001) treated mice, when compared to control mice. Accordingly, all treatments tested in this study were able to reduce microglia numbers in the striatum.

Next, we aimed to identify if the treatment dependent decrease in microglia is accompanied by a decrease in astrocytes. Therefore we counted GFAP positive cells, a marker traditionally used to label astrocyte populations under inflammatory conditions. One-way ANOVA analysis revealed significant differences of GFAP positive cells between treatment groups in the dorsal-lateral ($F_{(3,20)}$=11.84, p<0.001; Fig. 5E) and the ventral-medial ($F_{(3,20)}$=3.993, p<0.05; Fig. 5F) striatum. Post hoc analyses demonstrated that GFAP positive cells were decreased in amantadine (DL:

437 $p<0.01$), HU-308 (DL: $p<0.001$) and amantadine + HU-308 (DL: $p<0.001$; VM:
438 $p<0.05$) treated mice, when compared to control mice. Accordingly, all treatments
439 tested in this study were able to reduce astrocyte numbers predominantly in the
440 dorsal-lateral striatum.

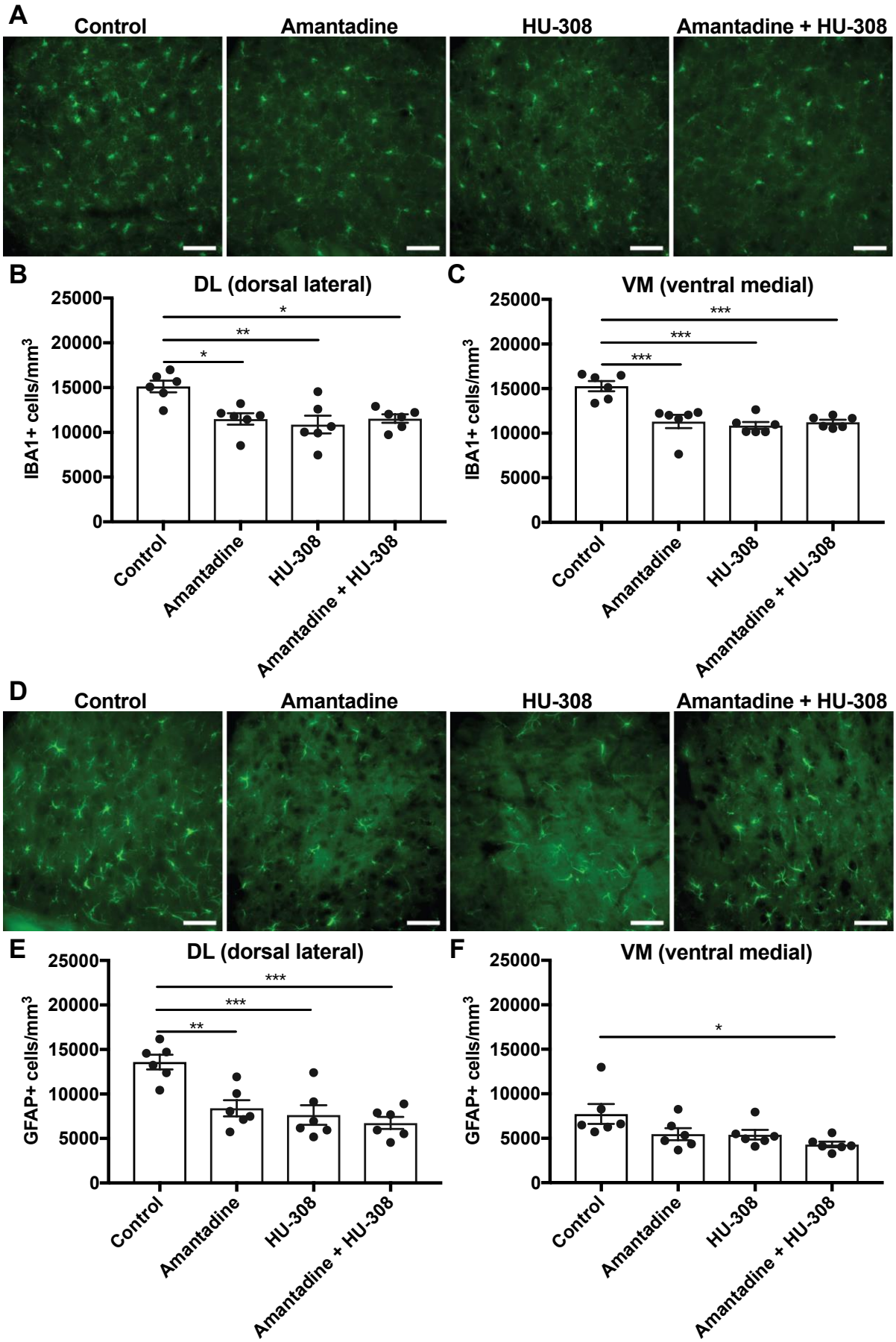
A
Control
Amantadine
HU-308
Amantadine + HU-308
B
DL (dorsal lateral)
IBA1+ cells/mm3
25000
20000
15000
10000
5000
0
*
**
*
Control
Amantadine
HU-308
Amantadine + HU-308
C
VM (ventral medial)
IBA1+ cells/mm3
***
***
***
Control
Amantadine
HU-308
Amantadine + HU-308
D
Control
Amantadine
HU-308
Amantadine + HU-308
E
DL (dorsal lateral)
GFAP+ cells/mm3
***
***
**
Control
Amantadine
HU-308
Amantadine + HU-308
F
VM (ventral medial)
GFAP+ cells/mm3
*
Control
Amantadine
HU-308
Amantadine + HU-308

441

Figure 5: Amantadine and HU-308 treatment regimes reduce microglia and astrocyte populations in the striatum of LID mice. Representative images for (A) IBA1+ and (D) GFAP+ cells in the ipsilateral striatum of different treatment groups. Stereological quantification demonstrated amantadine, HU-308, and amantadine + HU-308 treatments decreased IBA1+ cell counts in the (B) dorsal-lateral and (C) ventral-medial striatum and GFAP+ cell counts in the (E) dorsal-lateral and (F) ventral-medial striatum. All values represent the mean ± standard error of the mean (SEM). *** = $p < 0.001$, ** = $p < 0.01$, * = $p < 0.05$ compared to control group (n = 6 per group). Scale bar represents 50μm

3.2.2 Amantadine, HU-308 and combined treatment decreased cytokine expression in the striatum of dyskinetic mice

In addition to increasing in numbers, under inflammatory conditions microglia and astrocytes also upregulate their production of an array of cytokines. Accordingly, we next aimed to determine if amantadine, HU-308, and conjoint treatment can reduce the amount of pro-inflammatory cytokines (TNFα, IL-1β, IL-6) and/or alter an anti-inflammatory cytokine (IL-10) in striatal tissue via a bead-based immunoassay. One-way ANOVA analyses revealed significant differences in cytokine expression between treatment groups for TNFα ($F_{(3,28)}=3.675$, $p<0.05$; Fig. 6A) and IL-1β ($F_{(3,26)}=3.806$, $p<0.05$; Fig. 6B) but not IL-6 ($F_{(3,28)}=2.683$, $p=0.0659$; Fig. 6C) and IL-10 ($F_{(3,28)}=1.527$, $p=0.2293$; Fig. 6D). Post hoc analyses demonstrated that TNFα ($p<0.05$) and IL-1β ($p<0.05$) expression were significantly decreased in HU-308 treated mice when compared to control mice. Collectively these results indicate a treatment dependent reduction in pro-inflammatory but not in anti-inflammatory cytokines.

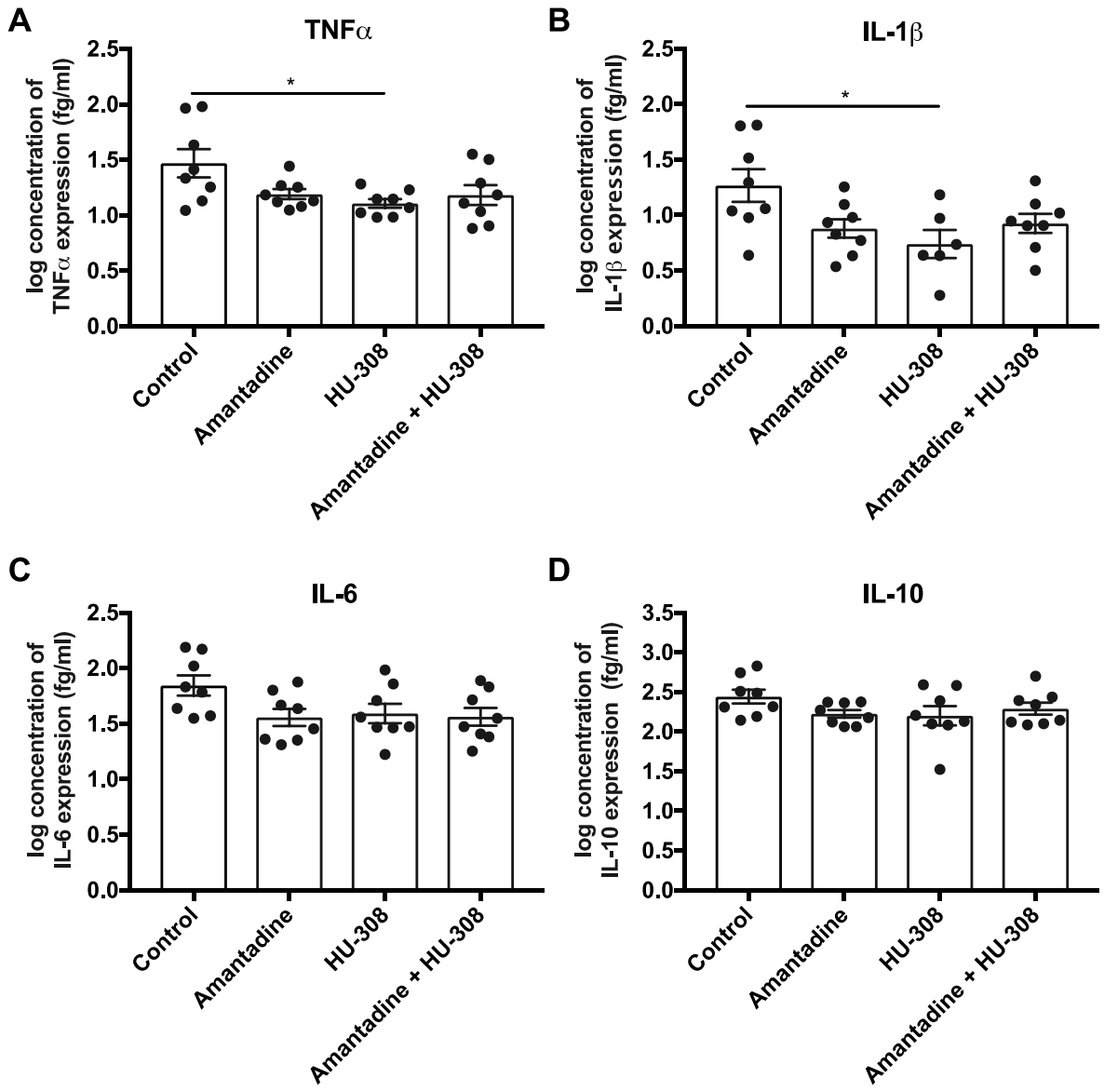

Figure 6. HU-308 treatment attenuates pro-inflammatory cytokine expression in the striatum of LID mice. HU-308 treatment significantly reduced (A) TNFα and (B) IL-1β expression, while no treatment regime had a significant effect on (C) IL-6 or (D) IL-10 expression as measured by bead-based immunoassay. All values represent the mean ± standard error of the mean (SEM). * = $p < 0.05$. (n = 6-8 per group).

3.2.3 Amantadine, HU-308 and combined treatment decreased NF-κB activity in the striatum of dyskinetic mice

The activity of the transcription factor NF-κB, a crucial regulator of the expression of several hundred target genes involved in inflammation and cell death, is upregulated in neuroinflammation. By measuring changes in expression of the phosphorylation site at Ser536, we aimed to determine increases in NF-κB activity across groups. One-way ANOVA analyses revealed significant differences of NF-κB(Ser536) ($F_{(3,28)}$=7.759, p<0.001; Fig. 7D) but not the total NF-κB protein ($F_{(3,28)}$=1.018, p=0.3995; Fig. 7B) between treatment groups. Post hoc analyses demonstrated that NF-κB(Ser536) was decreased in amantadine (p<0.001) and amantadine + HU-308 (p<0.05) treated mice, when compared to control mice.

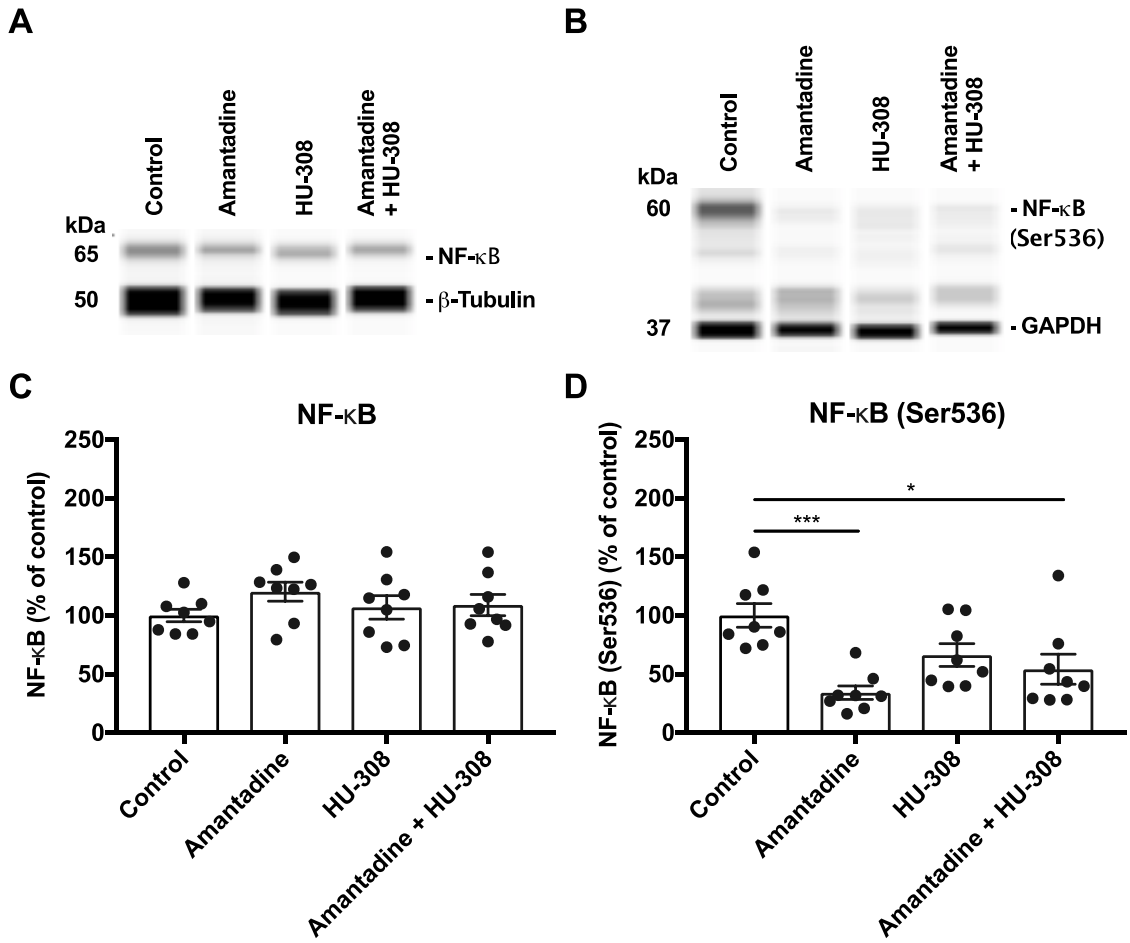

Figure 7: Amantadine treatment attenuates NF-κB activity in the striatum of LID mice

Representative pseudo bands generated by Wes of striatal (A) NF-κB and β-tubulin and (B) NF-κB(Ser536) and GAPDH expression. Western blotting quantification of (C) total NF-κB protein is unchanged in all groups, while (D) the NF-κB phosphorylation site Ser536 is significantly decreased in amantadine, HU-308 + amantadine treated mice when compared to control mice. All values represent the mean ± standard error of the mean (SEM). *** = $p < 0.001$, * = $p < 0.05$. (n = 8 per group).

4. Discussion

Throughout this study we have referred to the term neuroinflammation, which is classically defined by changes in glial proliferation, morphology and cytokine release, among other measures. However there has been an increasing recognition of the limitations of the term neuroinflammation and an increasing understanding of the multiple roles of glia in the healthy and diseased brain (Hammond et al., 2018; Khakh and Sofroniew, 2015; Morris et al., 2013). With this understanding, we and others have suggested that targeting glial homeostasis offers a promising route for treating neurodegenerative diseases and conditions in which synapse and neuron loss is implicated (Morris et al., 2013).

Given the evidence of altered glial function and morphology associated with LIDs (Mulas et al., 2016), the presence of CB2 receptors on glia, and their apparent effect of reversing altered glial function and morphology, (Benito et al., 2008), we hypothesised targeting CB2 receptors could provide a potential avenue for attenuating dyskinesia. Using a mouse model of LIDs, the current study revealed three key findings. First, the CB2 selective agonist HU-308 dose-dependently reduced LID to the same magnitude as the current frontline treatment, amantadine. Second, treatment with HU-308 plus amantadine resulted in an additive anti-dyskinetic effect. Third, these treatment regimens decreased the expression of neuroinflammatory mediators in the striatum of 6-OHDA lesioned mice. Our findings therefore provide the first evidence that targeting CB2 receptors may be a promising pharmacological strategy for alleviating LIDs, a major unmet clinical need for PD patients.

4.1 HU-308 dose-dependently reduced AIMs

To favor drug safety and tolerability, and to avoid adverse effects, cannabinoid treatments are preferably administered at the lowest therapeutically efficacious dose (MacCallum and Russo, 2018). Thus, we first determined the dose-dependent effect of HU-308 on reducing AIMs in a mouse model of LID. Our results suggest that 2.5mg/kg and 5mg/kg of HU-308 were able to reduce dyskinesia's to a similar extent, which is greater than that seen with 1mg/kg HU-308. Collectively, these results allow us to conclude that 2.5mg/kg HU-308 is an efficacious dose that achieves maximum reduction of AIMs in mice.

4.2 The anti-dyskinetic effect of HU-308 was CB2 specific

One major caveat for the therapeutic development of cannabinoids are the unwanted psychoactive side-effects associated with CB1 agonism (Pacher et al., 2006). A CB2 agonist offers a desirable alternative as it does not appear to trigger these side-effects (Tabrizi et al., 2016). HU-308 has previously been shown to be a CB2 specific agonist, efficiently binding to CB2 (K_i = 22.7), while not binding to CB1 (K_i > 10 μM) (Hanus et al., 1999). In order to test receptor specificity of drugs, it is common practice to demonstrate a lack of effect in receptor knockout animals. Although there are multiple CB2 knockout mouse lines available (Buckley et al., 2000; Li and Kim, 2016), CB2 lacking mice may be more susceptible to toxins, as evidenced by an increase in lesion severity in the LPS mouse model of PD (Gómez-Gálvez et al., 2016). Thus, the lesion size following 6-OHDA treatment would likely be larger in CB2 knockouts compared to wildtype controls which would affect the LID magnitude and make results difficult to interpret. Accordingly, as a consistent lesion volume is critical for our LID studies we were unable to use these genetically modified mice in our study. Therefore, in the current study we tested receptor

specificity by determining if the selective CB2 receptor antagonist SR144528 can block the anti-dyskinetic effect of the CB2 receptor agonist HU-308 administered only after the lesion is created. This strategy has previously been used in a rat model of Huntington's disease, with SR144528 blocking the neuroprotective effect of HU-308 (Sagredo et al., 2009). As hypothesized, SR144528 by itself had no effect on AIMs, but when administered in conjunction with HU-308, SR144528 fully blocked the anti-dyskinetic effect of HU-308. Together, these results allow us to conclude that HU-308's anti-dyskinetic properties are CB2 specific and unlikely due to any off-target effects.

4.3 The anti-dyskinetic effect of HU-308 is comparable to that of amantadine

After establishing the anti-dyskinetic efficacy of HU-308 we next aimed to compare the magnitude of this effect to that of amantadine. Others have previously reported that a dosage of 40mg/kg amantadine is close to the upper limit of its therapeutic efficacy in rodents (Brigham et al., 2018; Danysz et al., 1997). In our hands, amantadine at this dose resulted in a 30% reduction of AIMs and 45% reduction in FosB expression, which closely aligns with previous studies in 6-OHDA lesioned mice reporting the ability of amantadine to reduce both dyskinetic behavior (up to 36%) (Sebastianutto et al., 2016) and FosB expression (up to 47%) (Doo et al., 2014). This demonstrated the robustness of this model as a tool to detect improvements in LID symptoms. Remarkably, 2.5mg/kg HU-308 was as effective as amantadine and reduced AIMs by 31% and FosB expression by 50%. If it were to reproduce in human cohorts, pharmacologically targeting CB2 might provide a useful alternative to amantadine, for example in cases where there are amantadine specific side effects. In support of this, several CB2 selective agonists have shown to be safe, well tolerated, not associated with any major side effects, and effective in

578 treating peripheral pain and inflammatory conditions in Phase 1 and 2 clinical trials
579 (Di Marzo, 2018; Tabrizi et al., 2016). Accordingly, clinical trials investigating their
580 efficacy for neurodegenerative diseases is currently in high demand.

581 **4.4 HU-308 and amantadine have an additive anti-dyskinetic effect**

582 To maximize symptomatic relief it is common practice to treat patients with a
583 combination of different drugs (Thorlund and Mills, 2012). This is particularly
584 valuable where two drugs can act more effectively together such that the effect of the
585 two drugs in combination can exceed the maximal effect of either drug used alone.
586 We demonstrated that the anti-dyskinetic effect of HU-308 is dose-dependent, but
587 maximal at 2.5mg/kg. It is striking, therefore, that we found the addition of
588 amantadine to HU-308 treatment resulted in a greater magnitude of reduction in AIM
589 scores compared with that maximally achieved with HU-308. This result could be
590 taken to suggest that HU-308 and amantadine ultimately each modulate the
591 expression of LIDs through different but synergistic pathways so that the combined
592 effect of both exceeds that which can be achieved by HU-308 alone. Regardless, our
593 result suggests a combined HU-308 and amantadine treatment may be of greater
594 benefit for PD patients with LIDs than either alone.
595

596 **4.5 HU-308 and amantadine exert anti-inflammatory properties in striatal tissue**

597 In investigating the apparent effects of amantadine and HU-308 on glial responses in
598 this study we have largely confirmed previous published findings. In particular, it has
599 been reported that amantadine has effects on glia independently of its actions on
600 NMDA receptors, and that this is associated with the protection of cultured DA
601 neurons against MPP+ and LPS toxicity (Kim et al., 2012; Ossola et al., 2011) as
602 well the protection of TH+ neurons in an MPTP and LPS mouse model (Kim et al.,

2012). The latter study demonstrated amantadine treatment reduced microglia proliferation and decreased NF-κB activity (Kim et al., 2012). Our data confirms and advances these findings. Whereas previous studies focused on the impact of amantadine on neuroinflammation and related degeneration of dopaminergic neurons in the SNpc, we are the first to report that amantadine has the capability to reduce microglial proliferation, GFAP+ astrocytes and cytokine release in the striatum of dyskinetic mice.

Our experiments also confirm the effect of HU-308 in striatal tissue, as previously demonstrated in Parkinson's (Gómez-Gálvez et al., 2016) and Huntington's (Palazuelos et al., 2009) disease mouse models. In particular, those studies demonstrated that HU-308 treated mice showed a reduction in microglial proliferaiton and GFAP+ astrocyte populations in an excitotoxic Huntington's model (Palazuelos et al., 2009) and a reduction in activated microglia as well as reduced mRNA expression of the pro-inflammatory cytokines TNFα and IL-1β in an Parkinson's model (Gómez-Gálvez et al., 2016). Accordingly, our results strengthen the hypothesis of an anti-inflammatory protential of HU-308 acrross multiple neurodegenerative disorders and models.

4.6 HU-308 and amantadine did not exhibit an additive effect on neuroinflammation

Despite finding that both HU-308 and amantadine exert significant effects on glia in our model, we did not find an additive effect of combined treatment. This finding is not surprising as we (Morris et al., 2014, 2013) and others (Hammond et al., 2018; Khakh and Sofroniew, 2015) have previously suggested that microglia and

astrocytes are far more complex than previously thought. For example we now know that activated microglia drive the activation of astrocytes (Liddelow et al., 2017), that there are unique subsets of glia with only a proportion impacting neurodegenerative diseases (Deczkowska et al., 2018; Jordão et al., 2019; Keren-Shaul et al., 2017; Masuda et al., 2019) and that immediate activation and proliferation of microglia after neuronal injury may favour recovery (Tay et al., 2018, 2017). Accordingly, amantadine and HU-308 could be acting on some of these glial cell functions, and our broad measurements of glial cell counts and cytokines measurements only provide a small snapshot of the effects occurring in glia in our model.

Alternatively, the behavioural effect of each drug may be due, fully or in part, to effects of the drugs that are independent of their actions on dampening an inflammatory response associated with LIDs. For example, it has long been thought amantadine primarily suppresses LIDs via its weak NMDA antagonism (Blanpied et al., 2005; Paquette et al., 2012) on striatal neurons, which may be separate, additional to, or part of, its reported anti-inflammatory actions. Meanwhile, the well known presence of CB2 receptors on glia does not rule out a potential direct or indirect action on of CB2 receptor agonists at synapses. Indeed, activation of CB2 receptors in the hippocampus for 7-10 days increases mEPSC frequency and spine density, suggesting CB2 receptors may also function to modulate synaptic activity (Kim and Li, 2015). The latter finding could result from an indirect action of CB2 receptor activation on glia, since recent research suggests that glia regulate synapses in healthy conditions and in disease (Morris et al., 2013).

Our measures in this paper are too rudimentary to explore these various mechanisms, and much further research is needed. However, not withstanding this limitation, our data adds weight to the concept that agents that act on glia may provide a promising option in pre-clinical and clinical drug development for neurodegenerative diseases generally and for LIDs in particular.

4.7 Strengths, limitations and future directions

The current study had several strengths, supporting the robustness of our findings. First, we ensured that anti-dyskinetic effects were not due to coincidental allocation of mice with a lesser lesion into any one particular treatment group, by confirming TH levels in striatal tissue were not different between groups. Second, by conducting our study in mice with established LIDs (as described previously by us (Rentsch et al., 2019) and others (Sebastianutto et al., 2016)), mice were distributed so that there was no coincidental allocation of mice with lower or higher average AIM score in one or another group prior to treatment. Lastly, our behavioural data were largely correlated to the expression of FosB, a widely used molecular marker of LID (Andersson et al., 1999; Lundblad et al., 2004; Winkler et al., 2002). However, while this marker is mostly reliable in detecting gross changes in dyskinesia severity (dyskinetic vs. non-lesioned) it is possible this marker is unable to detect subtle to moderate changes within animals that are expressing dyskinesia (Smith et al., 2012). This may explain the instances in which FosB expression did not precisely corroborate our behavioural findings.

Our study also had limitations. As is often the case in preclinical research, our study was conducted in a homogenous population of adult male C57BL/6j mice. Thus, the

potential efficacy of HU-308 has not yet been assessed in cohorts with different ages, sexes and strains. These are important next preclinical steps, before translation is considered. Furthermore, while cannabinoid treatments shape as promising therapeutic targets for motor disorders, an important caveat is that cannabinoids might also act as motor-depressants. However, these effects are generally thought to be mediated by CB1 signaling, rather than CB2, which was one of the primary reasons we were interested in pursuing a CB2 agonist in this study (Hanus et al., 1999). In confirmation of this, in a previous study, HU-308 did not affect general motor activity in an open field test, nor did it cause catalepsy in naïve mice, even when administered at high doses (Hanus et al., 1999). Nevertheless, it will be important to conclusively determine if HU-308 has any effect on general or PD and LID specific motor activity in future studies. Finally, LIDs can last for many years in patients and we therefore suggest that, based on the enticing results of the current study, future studies of CB2 agonists in dyskinesias should confirm efficacy over a greatly extended period.

5. Conclusion

Collectively, our findings suggest CB2 agonists offer a putative target to treat LIDs, with efficacy comparable to the frontline treatment amantadine. This behavioural effect is associated with an effect on glial signalling (as evidenced by downregulation of neuroinflammation), providing further evidence that therapeutics targeting neuroinflammation and/or glial homeostasis may provide benefit for combating LIDs. Furthermore, one of the more important findings was the demonstration on an additive effect of HU-308 and amantadine that is greater than that achieved with HU-308 alone. Although we do not yet know the precise mechanisms driving this effect, our results suggest they may act by different but synergistic actions which has

important clinical implications. We have suggested several exciting future directions to investigate the mechanism by which amantadine and HU-308 may exert their effects, particularly exploring novel features of microglia and astrocyte physiology and pathophysiology and their direct and/or indirect impact on neuronal synaptic signalling which is known to be altered in dyskinesias. Our study suggests that targeting glial function may be an important strategy for developing therapies for treating LIDs, a major unmet need for PD patients.

Author contributions

Conceived and designed the experiments: PR SS BV. Performed the experiments: PR, TE. Analysed the data: PR SS. Contributed reagents/materials/analysis tools: BV. Wrote the paper: PR SS IC BV.

Acknowledgements

The authors would like to thank members of the Biological Testing Facility at the Garvan Institute for technical support and the members of the Centre of Neuroscience and Regenerative Medicine at the University of Technology, Sydney, for assistance in editing this manuscript. In particular we thank Dr. Gary Morris and Lyndsey Konen for constructive comments on the manuscript and helpful discussions.

Financial support

This work was supported by Helen and David Baffsky through the Helen and David Baffsky Fellowship to Sandy Stayte, as well as by Doug Battersby and family, David

King and family, Andrew Urquhart and family, Noel Passalaqua and family, and Parkinson's NSW. The funding sources had no involvement in the study design, collection or analysis or interpretation of data, writing of the manuscript, or in decision to submit the article for publication.

Declaration of interest

The authors have no conflicts of interest to declare.

References

Andersson, M., Hilbertson, A., Cenci, M.A., 1999. Striatal fosB Expression Is Causally Linked with l-DOPA-Induced Abnormal Involuntary Movements and the Associated Upregulation of Striatal Prodynorphin mRNA in a Rat Model of Parkinson’s Disease. Neurobiol. Dis. 6, 461–474. https://doi.org/10.1006/nbdi.1999.0259

Ashton, J.C., Glass, M., 2007. The cannabinoid CB2 receptor as a target for inflammation-dependent neurodegeneration. Curr. Neuropharmacol. 5, 73–80.

Ben Haim, L., Carrillo-de Sauvage, M.-A., CeyzÃ©riat, K., Escartin, C., 2015. Elusive roles for reactive astrocytes in neurodegenerative diseases. Front. Cell. Neurosci. 9, 278. https://doi.org/10.3389/fncel.2015.00278

Benito, C., Núñez, E., Tolón, R.M., Carrier, E.J., Rábano, A., Hillard, C.J., Romero, J., 2003. Cannabinoid CB2 receptors and fatty acid amide hydrolase are selectively overexpressed in neuritic plaque-associated glia in Alzheimer’s disease brains. J. Neurosci. 23, 11136–41.

Benito, C., Tolón, R.M., Pazos, M.R., Núñez, E., Castillo, A.I., Romero, J., 2008. Cannabinoid CB2 receptors in human brain inflammation. Br. J. Pharmacol. 153,

277–85. https://doi.org/10.1038/sj.bjp.0707505

Bisogno, T., Di Marzo, V., 2010. Cannabinoid receptors and endocannabinoids: role in neuroinflammatory and neurodegenerative disorders. CNS Neurol. Disord. Drug Targets 9, 564–73.

Blanpied, T.A., Clarke, R.J., Johnson, J.W., 2005. Amantadine Inhibits NMDA Receptors by Accelerating Channel Closure during Channel Block. J. Neurosci. 25, 3312–3322. https://doi.org/10.1523/JNEUROSCI.4262-04.2005

Booth, H.D.E., Hirst, W.D., Wade-Martins, R., 2017. The Role of Astrocyte Dysfunction in Parkinson's Disease Pathogenesis. Trends Neurosci. 40, 358–370. https://doi.org/10.1016/J.TINS.2017.04.001

Brigham, E.F., Johnston, T.H., Brown, C., Holt, J.D.S., Fox, S.H., Hill, M.P., Howson, P.A., Brotchie, J.M., Nguyen, J.T., 2018. Pharmacokinetic/Pharmacodynamic Correlation Analysis of Amantadine for Levodopa-Induced Dyskinesia. J. Pharmacol. Exp. Ther. 367, 373–381. https://doi.org/10.1124/jpet.118.247650

Buckley, N.E., McCoy, K.L., Mezey, E., Bonner, T., Zimmer, A., Felder, C.C., Glass, M., Zimmer, A., 2000. Immunomodulation by cannabinoids is absent in mice deficient for the cannabinoid CB(2) receptor. Eur. J. Pharmacol. 396, 141–9.

Cenci, M.A., Lundblad, M., 2007. Ratings of L-DOPA-induced dyskinesia in the unilateral 6-OHDA lesion model of Parkinson's disease in rats and mice. Curr. Protoc. Neurosci. Chapter 9, Unit 9.25. https://doi.org/10.1002/0471142301.ns0925s41

Chaudhuri, K.R., Healy, D.G., Schapira, A.H., 2006. Non-motor symptoms of Parkinson's disease: diagnosis and management. Lancet Neurol. 5, 235–245. https://doi.org/10.1016/S1474-4422(06)70373-8

Danysz, W., Parsons, C.G., Kornhuber, J., Schmidt, W.J., Quack, G., 1997.

779 Aminoadamantanes as NMDA receptor antagonists and antiparkinsonian agents
780 — preclinical studies. Neurosci. Biobehav. Rev. 21, 455–468.
781 https://doi.org/10.1016/S0149-7634(96)00037-1
782 Deczkowska, A., Keren-Shaul, H., Weiner, A., Colonna, M., Schwartz, M., Amit, I.,
783 2018. Disease-Associated Microglia: A Universal Immune Sensor of
784 Neurodegeneration. Cell 173, 1073–1081.
785 https://doi.org/10.1016/J.CELL.2018.05.003
786 Di Marzo, V., 2018. New approaches and challenges to targeting the
787 endocannabinoid system. Nat. Rev. Drug Discov. 17, 623–639.
788 https://doi.org/10.1038/nrd.2018.115
789 Doo, A.-R., Kim, S.-N., Hahm, D.-H., Yoo, H.H., Park, J.-Y., Lee, H., Jeon, S., Kim,
790 J., Park, S.-U., Park, H.-J., 2014. Gastrodia elata Blume alleviates L-DOPA-
791 induced dyskinesia by normalizing FosB and ERK activation in a 6-OHDA-
792 lesioned Parkinson's disease mouse model. BMC Complement. Altern. Med. 14,
793 107. https://doi.org/10.1186/1472-6882-14-107
794 dos-Santos-Pereira, M., da-Silva, C.A., Guimarães, F.S., Del-Bel, E., 2016. Co-
795 administration of cannabidiol and capsazepine reduces L-DOPA-induced
796 dyskinesia in mice: Possible mechanism of action. Neurobiol. Dis. 94, 179–195.
797 Fasano, S., Bezard, E., D'Antoni, A., Francardo, V., Indrigo, M., Qin, L., Doveró, S.,
798 Cerovic, M., Cenci, M.A., Brambilla, R., 2010. Inhibition of Ras-guanine
799 nucleotide-releasing factor 1 (Ras-GRF1) signaling in the striatum reverts motor
800 symptoms associated with L-dopa-induced dyskinesia. Proc. Natl. Acad. Sci. U.
801 S. A. 107, 21824–9. https://doi.org/10.1073/pnas.1012071107
802 Fernández-Trapero, M., Espejo-Porras, F., Rodríguez-Cueto, C., Coates, J.R.,
803 Pérez-Díaz, C., de Lago, E., Fernández-Ruiz, J., 2017. Upregulation of CB2

receptors in reactive astrocytes in canine degenerative myelopathy, a disease model of amyotrophic lateral sclerosis. Dis. Model. Mech. 10, 551–558. https://doi.org/10.1242/dmm.028373

Ferrer, B., Asbrock, N., Kathuria, S., Piomelli, D., Giuffrida, A., 2003. Effects of levodopa on endocannabinoid levels in rat basal ganglia: implications for the treatment of levodopa-induced dyskinesias. Eur. J. Neurosci. 18, 1607–14.

Fieblinger, T., Graves, S.M., Sebel, L.E., Alcacer, C., Plotkin, J.L., Gertler, T.S., Chan, C.S., Heiman, M., Greengard, P., Cenci, M.A., Surmeier, D.J., 2014. Cell type-specific plasticity of striatal projection neurons in parkinsonism and L-DOPA-induced dyskinesia. Nat. Commun. 5, 5316. https://doi.org/10.1038/ncomms6316

Finseth, T.A., Hedeman, J.L., Brown, R.P., Johnson, K.I., Binder, M.S., Kluger, B.M., 2015. Self-Reported Efficacy of Cannabis and Other Complementary Medicine Modalities by Parkinson's Disease Patients in Colorado. Evidence-Based Complement. Altern. Med. 2015, 1–6. https://doi.org/10.1155/2015/874849

Fox, S.H., Henry, B., Hill, M., Crossman, A., Brotchie, J., 2002. Stimulation of cannabinoid receptors reduces levodopa-induced dyskinesia in the MPTP-lesioned nonhuman primate model of Parkinson's disease. Mov. Disord. 17, 1180–1187. https://doi.org/10.1002/mds.10289

Girasole, A.E., Lum, M.Y., Nathaniel, D., Bair-Marshall, C.J., Guenthner, C.J., Luo, L., Kreitzer, A.C., Nelson, A.B., 2018. A Subpopulation of Striatal Neurons Mediates Levodopa-Induced Dyskinesia. Neuron 97, 787–795.e6. https://doi.org/10.1016/J.NEURON.2018.01.017

Gómez-Gálvez, Y., Palomo-Garo, C., Fernández-Ruiz, J., García, C., 2016. Potential of the cannabinoid CB2 receptor as a pharmacological target against

inflammation in Parkinson's disease. Prog. Neuro-Psychopharmacology Biol. Psychiatry 64, 200–208.

Gundersen, H.J., Jensen, E.B., 1987. The efficiency of systematic sampling in stereology and its prediction. J. Microsc. 147, 229–63.

Hammond, T.R., Robinton, D., Stevens, B., 2018. Microglia and the Brain: Complementary Partners in Development and Disease. Annu. Rev. Cell Dev. Biol. 34, 523–544. https://doi.org/10.1146/annurev-cellbio-100616-060509

Hanus, L., Breuer, A., Tchilibon, S., Shiloah, S., Goldenberg, D., Horowitz, M., Pertwee, R.G., Ross, R.A., Mechoulam, R., Fride, E., 1999. HU-308: a specific agonist for CB(2), a peripheral cannabinoid receptor. Proc. Natl. Acad. Sci. U. S. A. 96, 14228–33.

Javed, H., Azimullah, S., Haque, M.E., Ojha, S.K., 2016. Cannabinoid Type 2 (CB2) Receptors Activation Protects against Oxidative Stress and Neuroinflammation Associated Dopaminergic Neurodegeneration in Rotenone Model of Parkinson's Disease. Front. Neurosci. 10, 321. https://doi.org/10.3389/fnins.2016.00321

Jordan, C.J., Xi, Z.-X., 2019. Progress in brain cannabinoid CB2 receptor research: From genes to behavior. Neurosci. Biobehav. Rev. 98, 208–220. https://doi.org/10.1016/J.NEUBIOREV.2018.12.026

Jordão, M.J.C., Sankowski, R., Brendecke, S.M., Sagar, Locatelli, G., Tai, Y.-H., Tay, T.L., Schramm, E., Armbruster, S., Hagemeyer, N., Groß, O., Mai, D., Çiçek, Ö., Falk, T., Kerschensteiner, M., Grün, D., Prinz, M., 2019. Single-cell profiling identifies myeloid cell subsets with distinct fates during neuroinflammation. Science 363, eaat7554. https://doi.org/10.1126/science.aat7554

Keren-Shaul, H., Spinrad, A., Weiner, A., Matcovitch-Natan, O., Dvir-Szternfeld, R.,

Ulland, T.K., David, E., Baruch, K., Lara-Astaiso, D., Toth, B., Itzkovitz, S., Colonna, M., Schwartz, M., Amit, I., 2017. A Unique Microglia Type Associated with Restricting Development of Alzheimer's Disease. Cell 169, 1276–1290.e17. https://doi.org/10.1016/j.cell.2017.05.018

Khakh, B.S., Sofroniew, M. V, 2015. Diversity of astrocyte functions and phenotypes in neural circuits. Nat. Neurosci. 18, 942–52. https://doi.org/10.1038/nn.4043

Kim, J.-H.J., Lee, H.-W., Hwang, J., Kim, J.-H.J., Lee, M.-J., Han, H.-S., Lee, W.-H., Suk, K., 2012. Microglia-inhibiting activity of Parkinson's disease drug amantadine. Neurobiol. Aging 33, 2145–59. https://doi.org/10.1016/j.neurobiolaging.2011.08.011

Kim, J., Li, Y., 2015. Chronic activation of CB2 cannabinoid receptors in the hippocampus increases excitatory synaptic transmission. J. Physiol. 593, 871–886. https://doi.org/10.1113/jphysiol.2014.286633

Li, Y., Kim, J., 2016. Deletion of CB2 cannabinoid receptors reduces synaptic transmission and long-term potentiation in the mouse hippocampus. Hippocampus 26, 275–81. https://doi.org/10.1002/hipo.22558

Liddelow, S.A., Guttenplan, K.A., Clarke, L.E., Bennett, F.C., Bohlen, C.J., Schirmer, L., Bennett, M.L., Münch, A.E., Chung, W.-S., Peterson, T.C., Wilton, D.K., Frouin, A., Napier, B.A., Panicker, N., Kumar, M., Buckwalter, M.S., Rowitch, D.H., Dawson, V.L., Dawson, T.M., Stevens, B., Barres, B.A., 2017. Neurotoxic reactive astrocytes are induced by activated microglia. Nature 541, 481–487. https://doi.org/10.1038/nature21029

Lotan, I., Treves, T.A., Roditi, Y., Djaldetti, R., 2014. Cannabis (Medical Marijuana) Treatment for Motor and Non–Motor Symptoms of Parkinson Disease. Clin. Neuropharmacol. 37, 41–44. https://doi.org/10.1097/WNF.0000000000000016

879 Lundblad, M., Picconi, B., Lindgren, H., Cenci, M.A., 2004. A model of L-DOPA-
880 induced dyskinesia in 6-hydroxydopamine lesioned mice: relation to motor and
881 cellular parameters of nigrostriatal function. Neurobiol. Dis. 16, 110–23.
882 https://doi.org/10.1016/j.nbd.2004.01.007
883 MacCallum, C.A., Russo, E.B., 2018. Practical considerations in medical cannabis
884 administration and dosing. Eur. J. Intern. Med. 49, 12–19.
885 https://doi.org/10.1016/J.EJIM.2018.01.004
886 Manson, A., Stirpe, P., Schrag, A., 2012. Levodopa-Induced-Dyskinesias Clinical
887 Features, Incidence, Risk Factors, Management and Impact on Quality of Life.
888 J. Parkinsons. Dis. 2, 189–198. https://doi.org/10.3233/JPD-2012-120103
889 Martinez, A., Macheda, T., Morgese, M.G., Trabace, L., Giuffrida, A., 2012. The
890 cannabinoid agonist WIN55212-2 decreases l-DOPA-induced PKA activation
891 and dyskinetic behavior in 6-OHDA-treated rats. Neurosci. Res. 72, 236–242.
892 https://doi.org/10.1016/J.NEURES.2011.12.006
893 Masuda, T., Sankowski, R., Staszewski, O., Böttcher, C., Amann, L., Sagar,
894 Scheiwe, C., Nessler, S., Kunz, P., van Loo, G., Coenen, V.A., Reinacher, P.C.,
895 Michel, A., Sure, U., Gold, R., Grün, D., Priller, J., Stadelmann, C., Prinz, M.,
896 2019. Spatial and temporal heterogeneity of mouse and human microglia at
897 single-cell resolution. Nature 566, 388–392. https://doi.org/10.1038/s41586-019-
898 0924-x
899 Morgese, M.G., Cassano, T., Cuomo, V., Giuffrida, A., 2007. Anti-dyskinetic effects
900 of cannabinoids in a rat model of Parkinson’s disease: Role of CB1 and TRPV1
901 receptors. Exp. Neurol. 208, 110–119.
902 https://doi.org/10.1016/j.expneurol.2007.07.021
903 Morris, G.P., Clark, I.A., Vissel, B., 2014. Inconsistencies and Controversies

904 Surrounding the Amyloid Hypothesis of Alzheimer's Disease. Acta Neuropathol.
905 Commun. 2. https://doi.org/10.1186/s40478-014-0135-5
906 Morris, G.P., Clark, I.A., Zinn, R., Vissel, B., 2013. Microglia: A new frontier for
907 synaptic plasticity, learning and memory, and neurodegenerative disease
908 research. Neurobiol. Learn. Mem. 105, 40–53.
909 https://doi.org/10.1016/j.nlm.2013.07.002
910 Mulas, G., Espa, E., Fenu, S., Spiga, S., Cossu, G., Pillai, E., Carboni, E., Simbula,
911 G., Jadžić, D., Angius, F., Spolitu, S., Batetta, B., Lecca, D., Giuffrida, A., Carta,
912 A.R., 2016. Differential induction of dyskinesia and neuroinflammation by
913 pulsatile versus continuous l-DOPA delivery in the 6-OHDA model of
914 Parkinson's disease. Exp. Neurol. 286, 83–92.
915 https://doi.org/10.1016/J.EXPNEUROL.2016.09.013
916 Ossola, B., Schendzielorz, N., Chen, S.-H., Bird, G.S., Tuominen, R.K., Männistö,
917 P.T., Hong, J.-S., 2011. Amantadine protects dopamine neurons by a dual
918 action: reducing activation of microglia and inducing expression of GDNF in
919 astroglia [corrected]. Neuropharmacology 61, 574–82.
920 https://doi.org/10.1016/j.neuropharm.2011.04.030
921 Pacher, P., Bátkai, S., Kunos, G., 2006. The endocannabinoid system as an
922 emerging target of pharmacotherapy. Pharmacol. Rev. 58, 389–462.
923 https://doi.org/10.1124/pr.58.3.2
924 Palazuelos, J., Aguado, T., Pazos, M.R., Julien, B., Carrasco, C., Resel, E.,
925 Sagredo, O., Benito, C., Romero, J.J.J., Azcoitia, I., Fernández-Ruiz, J.,
926 Guzmán, M., Galve-Roperh, I., 2009. Microglial CB2 cannabinoid receptors are
927 neuroprotective in Huntington's disease excitotoxicity. Brain 132, 3152–64.
928 https://doi.org/10.1093/brain/awp239

929 Pandey, S., Srivanitchapoom, P., 2017. Levodopa-induced Dyskinesia: Clinical
930 Features, Pathophysiology, and Medical Management. Ann. Indian Acad.
931 Neurol. 20, 190–198. https://doi.org/10.4103/aian.AIAN_239_17
932 Paquette, M.A., Martinez, A.A., Macheda, T., Meshul, C.K., Johnson, S.W., Berger,
933 S.P., Giuffrida, A., 2012. Anti-dyskinetic mechanisms of amantadine and
934 dextromethorphan in the 6-OHDA rat model of Parkinson's disease: role of
935 NMDA vs. 5-HT1A receptors. Eur. J. Neurosci. 36, 3224–3234.
936 https://doi.org/10.1111/j.1460-9568.2012.08243.x
937 Pavón, N., Martín, A.B., Mendialdua, A., Moratalla, R., 2006. ERK Phosphorylation
938 and FosB Expression Are Associated with L-DOPA-Induced Dyskinesia in
939 Hemiparkinsonian Mice. Biol. Psychiatry 59, 64–74.
940 https://doi.org/10.1016/j.biopsych.2005.05.044
941 Paxinos, G., Franklin, K.B.J., 2001. The Mouse Brain in Stereotaxic Coordinates.
942 San Diego Acad. Press.
943 Perez-Lloret, S., Rascol, O., 2018. Efficacy and safety of amantadine for the
944 treatment of l-DOPA-induced dyskinesia. J. Neural Transm. 125, 1237–1250.
945 https://doi.org/10.1007/s00702-018-1869-1
946 Picconi, B., Centonze, D., Håkansson, K., Bernardi, G., Greengard, P., Fisone, G.,
947 Cenci, M.A., Calabresi, P., 2003. Loss of bidirectional striatal synaptic plasticity
948 in L-DOPA-induced dyskinesia. Nat. Neurosci. 6, 501–506.
949 https://doi.org/10.1038/nn1040
950 Price, D.A., Martinez, A.A., Seillier, A., Koek, W., Acosta, Y., Fernandez, E., Strong,
951 R., Lutz, B., Marsicano, G., Roberts, J.L., Giuffrida, A., 2009. WIN55,212-2, a
952 cannabinoid receptor agonist, protects against nigrostriatal cell loss in the 1-
953 methyl-4-phenyl-1,2,3,6-tetrahydropyridine mouse model of Parkinson's

disease. Eur. J. Neurosci. 29, 2177–86. https://doi.org/10.1111/j.1460-9568.2009.06764.x

Priller, J., Prinz, M., 2019. Targeting microglia in brain disorders. Science (80-.). 365, 32–33. https://doi.org/10.1126/science.aau9100

Rentsch, P., Stayte, S., Morris, G.P., Vissel, B., 2019. Time dependent degeneration of the nigrostriatal tract in mice with 6-OHDA lesioned medial forebrain bundle and the effect of activin A on l-Dopa induced dyskinesia. BMC Neurosci. 20, 5. https://doi.org/10.1186/s12868-019-0487-7

Sagredo, O., González, S., Aroyo, I., Pazos, M.R., Benito, C., Lastres-Becker, I., Romero, J.P., Tolón, R.M., Mechoulam, R., Brouillet, E., Romero, J., Fernández-Ruiz, J., 2009. Cannabinoid CB $_2$ receptor agonists protect the striatum against malonate toxicity: Relevance for Huntington's disease. Glia 57, 1154–1167. https://doi.org/10.1002/glia.20838

Schallert, T., Fleming, S.M., Leasure, J.L., Tillerson, J.L., Bland, S.T., 2000. CNS plasticity and assessment of forelimb sensorimotor outcome in unilateral rat models of stroke, cortical ablation, parkinsonism and spinal cord injury. Neuropharmacology 39, 777–787. https://doi.org/10.1016/S0028-3908(00)00005-8

Schuler, B., Rettich, A., Vogel, J., Gassmann, M., Arras, M., 2009. Optimized surgical techniques and postoperative care improve survival rates and permit accurate telemetric recording in exercising mice. BMC Vet. Res. 5, 28. https://doi.org/10.1186/1746-6148-5-28

Sebastianutto, I., Maslava, N., Hopkins, C.R., Cenci, M.A., 2016. Validation of an improved scale for rating l-DOPA-induced dyskinesia in the mouse and effects of specific dopamine receptor antagonists. Neurobiol. Dis. 96, 156–170.

https://doi.org/10.1016/J.NBD.2016.09.001

Sharma, V.D., Lyons, K.E., Pahwa, R., 2018. Amantadine extended-release capsules for levodopa-induced dyskinesia in patients with Parkinson's disease. Ther. Clin. Risk Manag. 14, 665–673. https://doi.org/10.2147/TCRM.S144481

Smith, G.A., Heuer, A., Dunnett, S.B., Lane, E.L., 2012. Unilateral nigrostriatal 6-hydroxydopamine lesions in mice II: predicting l-DOPA-induced dyskinesia. Behav. Brain Res. 226, 281–92. https://doi.org/10.1016/j.bbr.2011.09.025

Song, L., Yang, X., Ma, Y., Wu, N., Liu, Z., 2014. The CB1 cannabinoid receptor agonist reduces L-DOPA-induced motor fluctuation and ERK1/2 phosphorylation in 6-OHDA-lesioned rats. Drug Des. Devel. Ther. 8, 2173–9. https://doi.org/10.2147/DDDT.S60944

Stayte, S., Rentsch, P., Li, K.M., Vissel, B., 2015. Activin A protects midbrain neurons in the 6-hydroxydopamine mouse model of Parkinson's disease. PLoS One 10, e0124325. https://doi.org/10.1371/journal.pone.0124325

Stayte, S., Rentsch, P., Tröscher, A.R., Bamberger, M., Li, K.M., Vissel, B., Bamberge, M., Li, K.M., Vissel, B., 2017. Activin A inhibits MPTP and LPS-induced increases in inflammatory cell populations and loss of dopamine neurons in the mouse midbrain in Vivo. PLoS One 12. https://doi.org/10.1371/journal.pone.0167211

Suárez, L.M., Solís, O., Caramés, J.M., Taravini, I.R., Solís, J.M., Murer, M.G., Moratalla, R., 2014. L-DOPA treatment selectively restores spine density in dopamine receptor D2-expressing projection neurons in dyskinetic mice. Biol. Psychiatry 75, 711–22. https://doi.org/10.1016/j.biopsych.2013.05.006

Tabrizi, M.A., Baraldi, P.G., Borea, P.A., Varani, K., 2016. Medicinal Chemistry, Pharmacology, and Potential Therapeutic Benefits of Cannabinoid CB 2

Receptor Agonists. https://doi.org/10.1021/acs.chemrev.5b00411

Tay, T.L., Mai, D., Dautzenberg, J., Fernández-Klett, F., Lin, G., Sagar, Datta, M., Drougard, A., Stempfl, T., Ardura-Fabregat, A., Staszewski, O., Margineanu, A., Sporbert, A., Steinmetz, L.M., Pospisilik, J.A., Jung, S., Priller, J., Grün, D., Ronneberger, O., Prinz, M., 2017. A new fate mapping system reveals context-dependent random or clonal expansion of microglia. Nat. Neurosci. 20, 793–803. https://doi.org/10.1038/nn.4547

Tay, T.L., Sagar, Dautzenberg, J., Grün, D., Prinz, M., 2018. Unique microglia recovery population revealed by single-cell RNAseq following neurodegeneration. Acta Neuropathol. Commun. 6, 87. https://doi.org/10.1186/s40478-018-0584-3

Thiele, S.L., Chen, B., Lo, C., Gertler, T.S., Warre, R., Surmeier, J.D., Brotchie, J.M., Nash, J.E., 2014. Selective loss of bi-directional synaptic plasticity in the direct and indirect striatal output pathways accompanies generation of parkinsonism and l-DOPA induced dyskinesia in mouse models. Neurobiol. Dis. 71, 334–44. https://doi.org/10.1016/j.nbd.2014.08.006

Thiele, S.L., Warre, R., Nash, J.E., 2012. Development of a Unilaterally-lesioned 6-OHDA Mouse Model of Parkinson's Disease. J. Vis. Exp. 1–8. https://doi.org/10.3791/3234

Thorlund, K., Mills, E., 2012. Stability of additive treatment effects in multiple treatment comparison meta-analysis: a simulation study. Clin. Epidemiol. 4, 75–85. https://doi.org/10.2147/CLEP.S29470

Venderová, K., Růžička, E., Voříšek, V., Višňovský, P., 2004. Survey on cannabis use in Parkinson's disease: Subjective improvement of motor symptoms. Mov. Disord. 19, 1102–1106. https://doi.org/10.1002/mds.20111

1029 Walsh, S., Gorman, A.M., Finn, D.P., Dowd, E., 2010. The effects of cannabinoid
1030 drugs on abnormal involuntary movements in dyskinetic and non-dyskinetic 6-
1031 hydroxydopamine lesioned rats. Brain Res. 1363, 40–48.
1032 https://doi.org/10.1016/J.BRAINRES.2010.09.086
1033 Winkler, C., Kirik, D., Björklund, A., Cenci, M.A., 2002. l-DOPA-Induced Dyskinesia
1034 in the Intrastriatal 6-Hydroxydopamine Model of Parkinson's Disease: Relation
1035 to Motor and Cellular Parameters of Nigrostriatal Function. Neurobiol. Dis. 10,
1036 165–186. https://doi.org/10.1006/nbdi.2002.0499
1037 Zhang, Y., Meredith, G.E., Mendoza-Elias, N., Rademacher, D.J., Tseng, K.Y.,
1038 Steece-Collier, K., 2013. Aberrant restoration of spines and their synapses in L-
1039 DOPA-induced dyskinesia: involvement of corticostriatal but not thalamostriatal
1040 synapses. J. Neurosci. 33, 11655–67.
1041 https://doi.org/10.1523/JNEUROSCI.0288-13.2013
1042